Recent electrokinetic strategies for isolation, enrichment and separation of extracellular vesicles

Marco Morani, Thanh Duc Mai, Zuzana Krupova, Guillaume van Niel, Pierre Defrenaix, Myriam Taverna

Recent electrokinetic strategies for isolation, enrichment and separation of extracellular vesicles

Marco Morani[1], Thanh Duc Mai[1], Zuzana Krupova[2], Guillaume van Niel[3,4], Pierre Defrenaix[2], and Myriam Taverna[1,5*]

[1] Université Paris-Saclay, CNRS, Institut Galien Paris-Saclay, Protein and Nanotechnology in Analytical Science (PNAS), 92296, Châtenay-Malabry, France.

[2] Excilone - 6, Rue Blaise Pascal - Parc Euclide - 78990 Elancourt – France

[3] Université de Paris, Institute of Psychiatry and Neuroscience of Paris (IPNP), INSERM U1266, "Endosomal dynamic in neuropathies", F-75014 Paris,

[4] GHU PARIS Psychiatrie & Neurosciences, F-75014 Paris, France

[5] Institut Universitaire de France (IUF)

Correspondence: E-mail: myriam.taverna@u-psud.fr;

Keywords: capillary electrophoresis; electrokinetic approaches; extracellular vesicles; exosomes, isolation.

Abstract

Extracellular vesicles (EVs) are a family of cell-derived membrane vesicles that are present in almost all body fluids. EVs have gained significant interest over the last decades as mediators of key functions in numerous patho-physiological condition (clearance, signalling, trophic support, cargo delivery) and as potential prognostic or diagnostic biomarkers. The endogenous delivery capacities of these nanometric entities also hold a high potential as engineered drug nanocarriers for clinical and pharmaceutical applications, especially for targeted therapies. Nevertheless, knowledge about the features of individual EVs (composition, physical and chemical characteristics) is still at the infancy because of the technical challenges to purify and analyze the various subpopulations of EVs. In this review, a comprehensive overview of electrokinetically driven methods for isolation, enrichment and characterization of EVs is presented. This review covers new trends of analytical science (over 7 years up till 2020), serving for high-quality EVs production, isolation, analysis and quality control, which are expected to provide powerful and complementary alternatives to the conventional and recently emerged approaches such as microfluidics. We critically discuss here the pros and cons of the different instrumental and methodological developments for electrokinetic strategies applied to EVs.

1. Introduction

Extracellular vesicles (EVs) cover a family of heterogeneous particles delimited by a phospholipid bilayer and secreted by all types of cells, with a size ranging from around 30 nm up to a few micrometers. Based on existing knowledge of their biogenesis, EVs can be narrowly classified into two major groups: exosomes and microvesicles (see Fig 1 for EVs formation and secretion). However, these generic terms might mean different things depending on the research field [1]. For such reason, as endorsed by International Society of Extracellular Vesicles, “extracellular vesicles” is used as an umbrella term to represent all types of cell-secreted vesicles [2]. It is now well established that EVs are implicated in a wide range of physiological processes, such as immune response, tissue repair, inflammation and neuronal functions [3-5], as well as in different pathological processes, like diabetes, liver disease, neurodegenerative diseases and cancer progression [6-8]. As EVs and their composition reflects the patho-physiological state of their producing cells, they provide a new source of biomarkers for diagnostic and prognostic applications [9-12]. Their capacities to deliver encapsulated materials in a targeted way open new avenues to harness them as biocompatible drug nanovesicles in targeted therapies [13-16]. Depending on their cellular origin and state, EVs are highly miscellaneous in size, cargo and membrane composition [17]. Even though the past decades have witnessed an exponential development in the field of EVs, there is still a lack of widely accepted specific markers to characterize the different subpopulations of EVs. Moreover, guidelines for isolation, enrichment and separation of EVs samples are still facing difficulties to properly exclude contaminants and separate EV subpopulations. In this context, further investigations are required to improve isolation, enrichment and separation of extracellular vesicles in order to fully understand their intrinsic properties and to confirm their great potential in clinical applications.

EV isolation and enrichment is a prerequisite before their clinical use as diagnostic biomarker. A sufficiently high yield and good reproducibility of EVs purification / isolation process is required to get a representative batch of the whole EVs population and avoid unacceptably high batch-to-batch variations with evident failure at identification and validation of relevant biomarkers for instance. During the last years, many reviews have been dedicated to summarize and compare different technologies for isolation of EVs [18-26]. The traditional methods used for EV isolation exploit a variety of EVs properties, such as their density, shape, size, specific interaction with solvents and surface proteins (see Table 1 for comparison of the most commonly used EV isolation methods). Typical batch-wise isolation techniques include ultracentrifugation (UC), gradient ultracentrifugation, ultrafiltration, polymer co-precipitation, size-exclusion liquid chromatography (SEC), field flow fractionation and immunoaffinity. Among them, ultracentrifugation is the most widely used primary isolation method across all EVs applications (> 80 %) [27]. However, this approach has many disadvantages such as bulky and expensive equipment, time-consuming procedure, contamination by protein aggregates and other particles, as well as high-volume sampling. A comparison study on EVs isolation yields from human serum achieved with some of these conventional methods revealed the highest numbers of total isolated EVs for polymer-based precipitation and size-exclusion chromatography methods (*i.e.* 5.6×10^{10} and 4.2×10^{10} particles / mL according to NTA analysis, respectively) [28]. These were followed by ultracentrifugation and density gradient ultracentrifugation approaches that led to the obtention of EVs concentrations of between 3.8×10^{9} and 9.5×10^{9} particles / mL [28]. In parallel, microfluidic technologies have been recently exploited for EVs isolation, making use of both physical and biochemical properties of EVs at microscale level. Microfluidics offers a tremendous potential by minimizing the sample volume, cost and reagent consumption, performing the reactions faster and conducting multiple assays in small devices

simultaneously. These microfluidic systems bring also new functionalities and employ a wide range of EVs isolation approaches such as microporous filtration, immunoaffinity, trapping on nanowires, together with the use of acoustic, electrophoretic and electromagnetic sorting mechanisms [18, 19, 29-33].

Once EVs isolation has been achieved, it is also extremely challenging to verify the identity of EVs and monitor their quantity and quality. Until now, EVs characterization by multiple and complementary techniques has to be carried out to evaluate the performance of the isolation methods and to give an insight into the EV nature [21, 22, 34, 35]. Microscopy-based methods (transmission electron microscopy TEM, atomic force microscopy AFM), dynamic light scattering (DLS), nanoparticle tracking analysis (NTA), single EV analysis (SEA) method and tuneable resistive pulse sensing (TRPS) are among the most widely used to measure the physical characteristics of EVs. These methods and their inherent advantages and drawbacks for EVs detection / characterization are summarized in Table 2. Besides these techniques, conventional protein analysis techniques, such as Western blotting, enzyme-linked immunosorbent assay (ELISA) and mass spectrometry (MS), provide high-throughput mapping of EVs' membrane and intra-vesicular proteins. EVs also contain nucleic acids which can be successfully examined by conventional extractions such as phenol-based method and spin column techniques. This led to the development of DNA/RNA-detection-based analysis tools for EVs, notably polymerase chain reaction with real-time fluorescence measurements (RT-PCR) or more recent technologies such as Droplet PCR, Ion-Exchange Nano-detector and localized surface plasmon resonance (LSPR) based assay [21]. Among all conventional methods used for EV characterization, Western blotting (74 %), single particle tracking (72 %, mainly with NTA) and electron microscopy (60 %) are among the most widely used [27]. Microfluidic-based technologies have also evolved in the field of EV

detection, in which capture and characterization of EVs are combined in one integrated platform [29, 31, 32, 36]. These emerging approaches are expected to provide fast and sensitive measurement with little sample consumption.

In a related context, EVs have been considered as nanoparticles (NPs) since they are within the same size range. Among analytical methods commonly used for NP characterization, electrokinetic approaches have emerged as simple and powerful techniques that are complementary to other spectroscopic, microscopic and optical ones, providing supplementary information on NPs' electrophoretic mobility, ζ-potential, particle size and biomolecular interactions [37-40]. Indeed, microscale electrophoresis relying on electrophoretic migrations of charged species under a high electric field, with its notable advantages of high separation efficiency, limited consumption of sample/chemicals and high potential for miniaturization and integration, has been widely used for high-resolution separation, isolation as well as preconcentration of NPs. With a similar viewpoint, electrokinetic strategies are expected to provide a powerful tool / alternative to conventional methods for EVs production, analysis and quality control. By application of a (high) voltage, the negatively charged EVs can migrate at different mobilities according to their size, charge and shape. The electroosmotic flow (EOF), which is the bulk liquid motion normally occurred under a high voltage over a charged support, typically silica capillaries possessing negative surface charges, can also be used to tune the apparent mobilities of EVs. This mechanism can be exploited for either i) isolation of EVs (via a selective membrane for instance) from other untargeted entities (e.g. proteins, cell membrane debris) or ii) separation of EVs over a microchannel (capillary or microchip) (see Fig. 2 for schematic illustration). Both non-uniform electric fields (for dielectrophoresis) and uniform ones (for microscale electrophoresis), as well as different variants of electrophoresis (for instance isotachophoresis,

capillary zone electrophoresis etc.) can be used for these purposes. While both electrokinetic separation and isolation techniques rely on an electrical field to drive EVs, the migration pattern and geometric design of the system would determine the respective purpose (typically micro-bored channels for EVs microscale separation and chambers separated by membranes or porous supports for EVs isolation). Normally, high electrical fields (more than 300 V/cm) are required for the former whereas lower ones are employed for the latter. Herein, we report on the first comprehensive overview of different electrokinetic strategies for isolation, separation and quantification of EVs. These strategies that exploit the electrokinetic migration of EVs are expected to possess advantages over conventional approaches in term of high resolution for EVs separation, high purity for EVs isolation, high potential for miniaturization and integration, as well as high versatility (i.e. EVs isolation, separation and characterization using an electrical field). Different instrumental and methodological developments for such purposes as well as their positive features and limitations are discussed. There have been almost 35 research articles on this topic, with more than one-third released in the last two years (2019-2020), confirming the recent interest of our research community in this emerging approach to provide a reliable and accurate tool for purifying, characterizing and quantifying EVs.

2. A glance at EVs characteristics

It is widely accepted that the EVs size, contents and membrane composition are highly heterogeneous [5]. This heterogeneity relates partially to their origin and the patho-physiological state of the producing cells and will impact their different functionalities [41, 42]. Yet this heterogeneity is also dependent on various other factors. EVs indeed can vary widely in terms of their composition and may carry specific sets of proteins, lipids or RNA species that then determine their fate and functions [5, 43]. While the accumulating data in the

176 past few years indicated that all EVs possess a negative surface charge due to their negatively
177 charged phospholipid membrane, EVs from different origins may exhibit different zeta
178 potentials, varying from -10 to -40 mV [25]. The EVs concentrations also vary significantly
179 from one biofluid to another, from the range of 10^7 particles / mL for cerebrospinal fluid
180 (CSF) up to 10^8 -10^9 particles / mL for plasma and blood [25]. In addition, the number of EVs
181 released also changes depending on the physiological state of the parent cell and the
182 microenvironment conditions [44]. Similar to the behavior of cells, EVs are capable of
183 responding to changes in the microenvironment that surrounds them, resulting in EVs shape,
184 size and zeta potential variations in different buffer conditions [44, 45]. Zijlstra and Di Vizio
185 recently provided evidence that the heterogeneity of EVs is not only driven by size variation,
186 but also defined by their diverse proteomic profiles, N-Glycosylation patterns, lipidic, RNA
187 and DNA profiles [46]. All these data therefore suggest that while at first sight both EVs and
188 NPs were thought to share similar size and charge characteristics, a deeper investigation
189 revealed that EVs are much more complex than NPs and may behave differently from NPs
190 under an electric field [47].
191
192 Lysis and/or characteristic modification of EVs can also occur, requiring a careful and
193 restricted selection of suspension buffer composition and ionic strength during isolation and
194 analysis [48-50]. This suggests that numerous parameters must be considered when handling
195 the EVs, and high attention must be paid to maintain the native properties of EVs during
196 isolation, purification, characterization and quantification. It is well known that the
197 dependency of NPs' electrophoretic mobilities on their size, charge, charge-to-size ratio and
198 shape can be determined only under very specific conditions [51-54]. Various parameters,
199 notably background electrolyte (BGE) ionic strength, pH and composition as well as applied
200 electric fields were found to have impacts on NPs' electrophoretic mobilities [55]. The

situation is even more constrained for EVs. The fact that EVs from different origins probably have different shapes and also different proteins / biomolecules on their surface and that they are prone to lysis or shape-deformed renders it very difficult to establish rules for the sole dependency of EVs electrophoretic migration behavior on charge and/or size-based parameters. The application of a high electric field, as suggested by Jones *et al.* and d'Orlyé *et al.* when dealing with NPs [52, 56], may not be applicable for EVs because it would provoke EVs lysis. With the present state of the art of EV purification technologies, it is still not readily possible to obtain EVs with very low degree of polydispersity and narrow size distribution [47], whereas this is already possible for NPs synthesis. All these features imply that the solid background already acquired for NPs should be used with care when applying to EVs, and consideration of the difference between EVs' and NPs' behaviors should be taken into account when developing electrokinetic strategies for EVs production and characterization.

3. Electrokinetic isolation and enrichment of EVs

The utility of an electric field to isolate and manipulate EVs has been recently exploited as contact-free particle sorting mechanism within different developed microdevices. A summary of electrokinetic approaches for EVs isolation and enrichment is shown in **Table 3**. The electrophoretic sorting of EVs is based on different electric field intensity and charge-to-mass ratios of the EVs, without the need of pumps or other moving parts. Some of the devices presented here have proved the advantage of electrophoresis in EVs isolation via a filtration mode. In this sense, Davies et al. demonstrated direct isolation of EVs from mouse's whole blood [57]. In this system, they designed a porous polymer monolith in the center of an open cross flow channel to act as a membrane filter. This nano-pored monolithic membrane, playing the role of a size exclusion filter, was prepared in situ and was integrated into a

poly(methyl methacrylate) micro-system. To render the monolithic membrane compatible with the extraction of vesicles, pore size was tuned to fit EVs sizes by changing the ratio of porogenic solvent to monomer solution. Then, direct current (DC) electrophoresis with a bias voltage of 10V (corresponding to an electric field of 6.25 V/cm) was activated with the electric field applied perpendicular to the flow direction to propel the EVs across the membrane and drive them in the opposite direction to the positively charged interfering large debris and proteins, thus avoiding the clogging that occurred when simple pressure-driven mode is employed (see Fig 3 for comparison between pressure-driven and electrokinetically-driven EVs isolation). In this configuration, sample and collection streams were performed at a relatively high flowrate (2 µl/min) to prevent larger particles and cells in the bulk stream from retaining onto the membrane. EVs extraction from 240 µL of blood could be completed within 2 hours using this system. A 10-fold better purity of isolated EVs (approaching the purity offered by ultracentrifugation) was achieved when compared to that obtained with the pressure-driven mode. Moreover, the electrophoresis mode demonstrated the capacity to remove most of the soluble proteins from mouse blood, similarly to conventional ultracentrifugation. Nevertheless, the EVs recovery with this electrokinetic mode was unsatisfactory, with only 2% of EVs recovered. In another microdevice isolation system, Cho et al. applied a higher electric field across a porous dialysis membrane with an appropriate pore size (30 nm) to selectively capture EVs on the membrane from mouse blood plasma while facilitating protein migration through the membrane [58]. In this isolation system, two electrodes and two membranes between electrodes are juxtaposed. Three flow channels were arranged between electrodes and membranes, one for sample solution, one for cathodic buffer, and the other for anodic buffer. EVs and other particles (e.g., proteins) move horizontally in the sample flow confined between the membranes, and simultaneously migrate vertically under the applied voltage. As EVs and most of the proteins in the plasma (e.g., albumin) have

negative surface charges, they move toward the anode and encounter the membrane, whereas particles with neutral or positive charges (e.g., histidine, lysine, non-polar lipids) move with the sample flow or are driven toward the cathode by electrostatic attraction. When the negatively charged particles arrive at the membrane pores, only small species (i.e., proteins) can pass through the membrane to enter the buffer channel and are consequently flushed out. In contrast, particles > 30 nm (i.e., EVs) accumulate on the membrane, and the attached EVs are then washed and collected by pipetting with phosphate buffered saline (PBS). The membrane can be regenerated after each EVs collection for repeated use. Based on NTA measurements, this method permitted a 65% EVs recovery rate in approximatively 30 minutes. According to RNA analysis and characteristic EV protein (CD63), this device led to less impurities than commercial polyethylene glycol (PEG) precipitation method (84 % vs 68 %, respectively). However, EVs isolated using this technique were less pure than those isolated by conventional ultracentrifugation (98 %).

In a related context, Mogi et al. proposed in 2018 the use of an electrical filtration device utilizing an ion-depletion zone in a microchannel to concentrate EVs from the culture media of four types of cell lines [59]. The approach is called ion concentration polarization (ICP). Readers can refer to a recent review for the theoretical background and extended applications of this electrokinetic concentration mode on chips utilizing ICP [60]. The ion-depletion zone, from which all positively and negatively charged particles are excluded, was generated by applying a voltage between two microchannels, i.e. main and ground (GND) channels, bridged by a cation-exchange membrane. The application of a voltage caused cations around the bridged area of the high-voltage side in the main channel to be drawn into the low-voltage zone of the GND one, resulting in an increase in the anions' amount relative to the cations' one. This led to an instantaneous expulsion of anions by electrostatic repulsion to re-establish

the electro-neutral situation, thereby forming an ion-depletion zone. As long as the electrostatic force required to generate the ion-depletion zone is still stronger than the driving force needed to move particles into the zone, the ion-depletion zone works as an intangible barrier to prevent any charged particles from entering in this zone. As a result, any negatively charged particles (more specifically EVs) passing through this zone by a pressure-driven flow are pushed away to the other side of the microchannel for preconcentration / collection (see Fig 4). They demonstrated that the ion-depletion zone method caused less damage to EVs when compared to standard ultracentrifugation isolation process. The EV recovery yields achieved for ICP and ultracentrifugation isolation were 98 % and 57 %, respectively. Further evidence is of course needed to certify the potential of the former for EVs concentration and separation from clinical samples. Interestingly, the ion depletion feature was also exploited in the same year by Marczak *et al*. These authors designed a different electrophoresis assisted device for EVs isolation that uses a cation-selective membrane to produce a transverse local electric field [61]. Under this electric field, the EVs pumped with a syringe into the microchip were carried into a perpendicular channel containing agarose gel, which filtered undesirable cell debris, and finally got concentrated near the membrane surface. When tested with cell culture media and blood sample spiked with EVs isolated with a commercial kit, this device was able to isolate between 60% and 80% of the incoming EVs within 20 min. This system demonstrated a superior recovery yield compared to the conventional techniques of ultracentrifugation (6 %) and polymer-based precipitation (ExoQuick, 30 %). Furthermore, the use of negatively charged membranes allowed prevention of membrane pore clogging by repelling the exosomes, whereas the utilization of the external ion concentration polarization phenomenon enriched these target entities. Later, Cheung *et al.* exploited the use of ion-selective membranes as well, by printing them directly on a PMDS microchannel [62]. This system incurred surface binding-based or passive trapping mechanism near the conductive

polymer membrane, allowing to simultaneously preconcentrate and capture EVs. The buffer solution was loaded into the cathodic reservoir and allowed to flow through the channel, whereas the EV sample was loaded into the anodic reservoir. Once the voltage was applied (electric field of 45 V/cm), the flow generated by the electroosmotic flow (EOF) pushed the EVs towards the cathode reservoir in front of the printed membrane. This ICP-based electrokinetic concentrator was demonstrated to preconcentrate and capture EVs from human breast cancer cell lines by increasing the EVs concentration by ~100-fold within 30 min. The limit of detection achieved was 5 x 10^7 particles / mL, which is better by two orders of magnitude than those obtained with a microfluidic approach without ICP. Their fabrication strategy that decoupled the ion-selective membrane from the substrate allowed the flexibility of either using an antibody-immobilized substrate to increase the EVs capture specificity or a glass substrate with passive microtraps to capture EVs in a highly efficient manner. However, once again, the EVs samples tested with this system came from batches extracted using a commercial kit. Direct application of this device to untreated clinical samples has yet to be demonstrated.

Diverted from DC electrophoresis driven mechanism, a nonuniform electric field was combined with immunoaffinity strategy for isolation of EVs [63]. Vaidyanathan et al. developed a microfluidic device containing a long array of asymmetric functionalized electrode pairs within three individual microfluidic channels. The use of an alternating current across the electrodes generated flow vortices that both increased collisions between target EVs and functionalized electrodes and reduced nonspecific adsorption of weakly bound molecules from the electrode surface. Detection and quantification of EVs spiked in PBS and breast cancer patient serum were performed both visually and via absorbance measurements from colorimetric solutions. A 3-fold enhancement in detection sensitivity compared to a

pressure-driven system (via a syringe pump) was reported. On the other hand, considering that it is closer to an immunoaffinity based method, it could only capture EVs expressing a given specific antigen, potentially excluding other EVs subpopulations concurrently present in a biofluid.

At a glance, electrokinetic strategies exhibit relatively higher EVs recovery yields (varying between 60 - 98 %, depending on the working principle) compared to those obtained with conventional precipitation (30 %) and ultracentrifugation (6 % - 57 %, depending on testing conditions). Better purities are also achieved with electrokinetic approaches. Among all approaches presented, the electrophoretic isolation on porous membranes and ICP-based gel electrophoresis offered the highest EV isolation yield, which is far superior than those of conventional methods. This technique [61], however, may come with a penalty of large size distribution up to 400 nm. On the other hand, much narrower size distribution was achieved with the ICP system [59], but further tests using clinical samples need to be performed in terms of EVs recovery and purity compared to conventional approaches. Note that a fair and systematic comparison of EVs isolation performances between electrokinetic strategies, microfluidic ones and the established methods (i.e. ultracentrifugation, polymer precipitation, membrane filtration, size exclusion chromatography SEC and membrane affinity) could not be made at the actual stage, as electrokinetic and microfluidic approaches are still under development and considered as emerging trends. They are therefore not included yet in different systematic performance evaluation / comparison studies. To have a rough estimation, readers can nevertheless glean to a recent study by Tian et al. for information on the EVs isolation performance of different established methods [64]. Starting from a same platelet-free plasma sample, ultracentrifugation is first ranked for the purity of isolated EVs (78 %), followed by SEC (28 %) and polymer precipitation (5 - 18 %). On the contrary, the yields

provided by polymer precipitation kits (83-89 %) are much higher than those obtained with SEC (65 %) and ultracentrifugation (2 %). The presence of electrokinetic strategies in such comparison study is expected soon to appear.

4. Electrokinetic separation and quantification of EVs

4.1. Dielectrophoresis of EVs

The reported electrokinetic strategies for separation and quantification of EVs are summarized in **table 4**. Dielectrophoresis (DEP) was the first approach developed for such purpose. DEP is the motion mechanism of an electrically polarizable particle that occurs in the presence of a non-uniform electric field [65]. Upon generation of a non-uniform electric field, the movement of charged particles driven by the dielectric force depends on their size and dielectric properties, the electrical properties of the suspending solution as well as the frequency and intensity of the applied electric field. DEP was employed to manipulate EVs after successful application with microparticles, nanoparticles and cells [66-68]. The DEP separation force generated by the alternating current electrokinetic (ACE) microarray chip device was first demonstrated in 2017 by Ibsen et al. for rapid isolation and recovery of glioblastoma EVs spiked in human plasma in less than 30 min [69]. The setup of this system is illustrated in Fig. 5. On the ACE chip, the EVs were attracted to the high-field regions around the microelectrode edges, while cells or larger particles in the samples were concentrated into the DEP low-field areas between the microelectrodes. The attracted EVs were either observed under SEM and detected by fluorescent staining after washing away the excess plasma or eluted from the chip and collected for further analysis. Nevertheless, protein aggregates and other cellular debris were undesirably collected as well. The same ACE procedure was then applied for capture and analysis of EVs from whole blood, plasma and serum of pancreatic ductal adenocarcinoma (PDAC) patients [70]. Two EV associated

proteins of interest, glypican-1 and CD63, were subsequently detected and measured using immunofluorescence-based methods to distinguish between PDAC patients from healthy controls with 99% sensitivity and 82% specificity. However, it was not clear whether the high levels of glypican-1 and CD63 were caused by elevated protein-to-exosome ratio or increased number of exosomes. In another study, Shi et al. reported a dielectrophoretic approach to design an insulator-based dielectrophoresis (iDEP) to capture EVs at the proximity of a glass nanopipette tip using a DC field [71]. The instrumental setup is shown in Fig. 6, in which a nanopipette was inserted into the opening of a chamber and connected with platinum electrodes. This device was based on the application of negative voltage polarity at the base of the pipette and induction of a strong non-uniform electric field that created a DEP force near the pipette region. The EVs trapping was controlled by three dominant forces including dielectrophoretic, electrophoretic and electroosmotic ones. The separation performance was first confirmed with fluorescence intensity measurements using fluorescently labelled artificial liposomes in PBS solution to simulate EVs capture. The separation capability of this iDEP device was further demonstrated in an extended setup connecting four micropipettes in parallel on a single chip, to carry out the extraction of EVs within 20 minutes from 200 μL of undiluted human plasma, serum or saliva [72]. According to NTA results, this method showed two orders of magnitude greater yields when compared to the differential centrifugation method, with a particle size distribution ranging from 50 nm to 150 nm covering most of the small and large EV subpopulations. This yield improvement came with a penalty of larger initial sample volumes needed. Ayala-Mar et al. then designed another direct current–insulator-based dielectrophoretic (DC-iDEP) system not only for EVs capture but also for EVs separation and collection based on their size [73, 74]. This device is composed of a microchannel having two different electrically insulating post sections, each with different gap space (15 μm and 10 μm). Adjacent to these two sections, side channels with recovery

reservoirs are arranged to allow collection of the separated sample. When DC voltages are applied, the EVs are dragged by the EOF across the main channel. As a result, large EVs are captured in the first post array, while smaller size EVs are trapped in the second post array. DLS measurements of two recovered fractions demonstrated successful separation of two different EV sizes of approximatively 120 nm and 75 nm in only 20 s. Furthermore, such a tool was able to concentrate and separate EVs from previously extracted EV samples. Chen et al. then gave an account of the development of a fast DEP method to isolate EVs with higher yield (>87%) and higher purity than conventional ultracentrifugation from plasma [75]. This DEP chip consisted of interdigitated electrodes covered with poly-HEMA hydrogel to reduce their degradation by the contact with high conductivity samples. Under positive DEP force, the EVs were successfully attracted and concentrated near the edges of the microelectrodes. The DEP step was followed by *in situ* lysis of EVs for identification of miRNAs levels in lung cancer patients. In addition, the authors demonstrated with DEP chips the possibility of *in situ* siRNA loading by electroporation of EVs that could be exploited for drug delivery and/or gene therapy. To conclude this section, the dielectrophoretic-based methods presented here demonstrate label-free, rapid and high-throughput separation of EVs. However, in our opinion, only few devices proved to be able to concentrate and separate EVs from complex biological mixtures. Pre-treatment of biological samples was always needed as forefront of these DEP approaches. Integration of upstream sample processing to downstream DEP-based separation of EVs should be envisaged and constitutes probably attractive perspectives to improve the performance of these systems in the future.

4.2. Microscale electrophoresis of EVs

During the past decade, microscale electrophoresis has been explored to provide analysis and characterization of EVs and potentially distinguish EV subtypes based on their electrophoretic

migration in a microchannel under a high intensity electric field. The first electrokinetic approach coupled with light-scattering-based detection was reported in 2013 by Ichiki's group for tracking EVs and obtaining their zeta potential, using an on-chip microcapillary electrophoresis (μCE) system coupled with a laser dark-field microscope [76-79]. A typical setup is shown in Fig. 7. This μCE consisted in a microfluidic channel in which EVs flow under application of DC voltage and afterwards they are tracked thanks to a laser dark-field microscope. This system enabled individual EVs visualization in a dark field by detecting the scattered laser light and their zeta potential was deduced from the measured electrophoretic mobility, revealing a strong correlation between the EVs zeta potential and their cells of origin. Furthermore, the authors developed an on-chip immunoelectrophoresis method to profile the protein expression of individual EVs, detecting their shifts in the electrophoretic velocity which resulted from the binding of EVs to specific antibody markers. This system was expected to be a valuable tool for sensitive profiling of EVs of tumor origin and therefore for early cancer diagnosis. Nevertheless, specific purpose-made instrumentation and manual operation are required for this new application, hindering its high throughput potential.

Diverted from the microchip setup, Lan et al. reported the first result of a capillary electrophoresis (CE) method applied for urinary EVs [80]. The authors investigated the potential of CE for separation of two kinds of EVs exhibiting different densities and obtained by sucrose gradient ultracentrifugation. However, it was not clear if the peaks detected from the CE analysis of low- and high- density EVs were either a result of different EVs size or different charge characteristics related to their different origins. No concrete information could be withdrawn from this work, due to (at least partially) the non-optimized conditions employed for CE analysis of EVs. More recently, two capillary electrophoresis methods have been proposed for the identification and quantification of EVs after their isolation. Piotrowska

et al. demonstrated a CE-UV method for qualitative and quantitative analysis of bacterial EVs [81]. To maintain EVs stability during CE analysis under electric field, the authors employed large buffering counter-ions. Thanks to this configuration, they obtained satisfactory separation of EVs from other non-target entities / molecules without any sample pretreatment in about 15 minutes, using the optimized BGE composed of 50 mM 1,3-Bis(tris(hydroxymethyl)methylamino)propane (BTP) and 75 mM glycine (pH 9.5) and application of an electric field of 333 V/cm. This method coupled with UV detection at 200 and 230 nm enabled the identification and quantification of EVs in the samples featuring protein concentration down to 0.17 mg/mL. Although this method enabled to quantify the number of vesicles in isolates, the linear correlation achieved was far from optimal (R^2 = 0.81) due to the presence of co-isolated impurities and the lack of a standard for method validation. Furthermore, the ability of this CE-UV method to separate and distinguish EVs from different origins was not investigated. In a parallel work, Morani et al. proposed a CE method with a laser-induced fluorescent (LIF) detection for the electrokinetic profiling of EVs from different sources (animal and human fluids) [47]. In this approach, EVs were first rendered fluorescent via an intra-membrane labeling. The CE-LIF separation of labelled EVs from the residual fluorophore was performed under an electric field of 500 V/cm. A new BGE was proposed for such purpose, employing large and weakly charged molecules (i.e. Tris(hydroxymethyl)aminomethane and N-Cyclohexyl-2-aminoethanesulfonic acid) at extremely high concentrations to avoid / minimize adsorption of EVs onto the silica capillary wall and lysis of EVs during electrophoresis. To avoid aggregation of EVs, buffer substitution of the analyzed samples was performed to avoid the high conductivity of the PBS matrix of the samples. A protocol overview and a typical electropherogram are shown in Fig. 8. Unlike UV detection, LIF detection offered better sensitivity achieving a detection limit of approximatively 8×10^9 EVs / mL (i.e. 5-fold better than the CE-UV approach) that is

476 sufficient for this method to be used for quality control of EVs batches isolated with different
477 conventional EV isolation techniques. Despite the additional fluorescent labelling step to
478 render the EVs detectable with a LIF detection, no morphology modifications of EVs were
479 produced according to DLS and NTA data. This CE-LIF method allowed to reveal different
480 profiles and electrophoretic mobilities for isolated EVs from different origins. However,
481 further characterization study is needed to prove whether such differences are size-dependent
482 or due to different surface composition. Different from the intra-membrane labelling strategy
483 for CE-LIF of EVs, Tani and Kaneta have very recently proposed an alternative for LIF-based
484 quantification of exosomes, using indirect capillary electrophoresis immunoassay (CEIA) of
485 exosomal membrane protein, CD63 [82]. In this method, reactions between the exosomes and
486 a fluorescently labeled anti-CD63 antibody were optimized to form a CD63 complex
487 localized on the surface of exosomes, followed by removal of the exosome-antibody complex
488 by centrifugation prior to CE-LIF analysis of the supernatant containing the free fluorescent
489 antibody. The diminution of peak areas was proportional to the increase in EVs' amount when
490 the initial fluorescent antibody's concentration was kept constant. Thus, the concentration of
491 the exosomal membrane's CD63 could then be estimated based on the slope of the linear
492 relationship. This "indirect" method that measures the concentration of the fluorescent
493 antibody allows straightforward quantification of exosomes without possible interference of
494 unwanted peaks. Nevertheless, no information on the electrokinetic profile reflecting the size /
495 charge distribution and eventual presence of EVs subpopulations can be provided this way.
496 Detection bias can also occur if membrane debris are co-present in the EVs sample.
497
498 ***4.3. Other related techniques***
499 In addition to the electrokinetic strategies listed above, other techniques have also been
500 investigated. Petersen et al., for instance, presented a cyclical electric field flow fractionation

501 (Cy-El-FFF) approach to separate EVs based on their size and charge [45]. Basically,
502 application of an AC voltage produces a strong electric field perpendicular to the direction of
503 flow, which enables EVs separation within a channel, due to their different electrophoretic
504 mobilities. This strategy showed changes in electrophoretic mobilities when similarly sized
505 polystyrene particles, melanoma exosomes sourced from a common human A375 melanoma
506 cell line or synthetic liposome-based exosome mimetics were substituted in different buffers
507 (i.e. deionized water, PBS, trehalose and isopropyl alcohol) having different salt
508 concentrations. Therefore, EVs could be separated depending on their different charge in
509 different buffers. In another work, Al Ahmad et al. reported an electrical detection and
510 quantification of EVs via capacitance-voltage measurements [83]. The authors compared
511 three types of EVs and demonstrated the identification of EVs according to their
512 corresponding self-capacitance. However, the employed equipment in this work enabled only
513 to estimate the EVs count. This could be overcome in the future by implementation of more
514 precise micro/nano-based capacitance analysers. Recently, Akbarinejad proposed a new
515 approach relying on a low electric field and an electrochemically switchable substrate for the
516 fast, selective, nondestructive, and efficient capture and release of EVs [84]. In this system,
517 using gold-sulfur (Au-S) covalent bonding, the electrospun substrates were functionalized
518 with SH-terminated aptamer probes that are selective to EV surface proteins. The specific
519 aptamer–EV interactions allows efficient capture of EVs and easy removal of the
520 nonspecifically bound material through washing steps. The trapped EVs were then released
521 into fresh PBS at a high efficiency (> 92 %) by applying a potential of −1.2 V for 5 min for
522 cathodic cleavage of the Au–S bond. This approach was demonstrated for capture, enrichment
523 and release of EVs derived from primary human dermal fibroblast (HDFa) and breast cancer
524 (MCF-7) cell lines with low nonspecific adsorption.
525

A high resolution particle-to-particle measurement technique, developed by Trau et al. for nanoparticle characterization [85, 86] and commercialized under a trade name of qNano – Izon Science [87], has recently been adapted for measurements of EVs' size, volume and surface charge. This elastic pore sensor, employing the tunable resistive pulse sensing (TRPS) principle is composed of conically shaped, size-tunable pores that are fabricated by puncturing a polyurethane thermoplastic membrane with a tungsten needle. Stretching or relaxing the elastic membrane allow the dimensions of the conical pore to be tuned to the size range of the target particles. When a voltage is applied across the conical pore, its shape results in a resistance gradient. TRPS measures nanoparticles suspended in electrolytes on a particle-by-particle basis as they pass through a nanopore. Sample particles are driven through the nanopore via a combination of pressure and voltage. Each particle causes a resistive pulse or "blockade" signal that is detected and measured. The blockade magnitude is directly proportional to the volume of each particle. The blockade duration is dependent on the velocity and surface charge of the particle, and blockade frequency is used to determine particle concentration. Applications of this technology have been extended recently to measure physiochemical parameters (size, concentration and charge) of EVs and nanomedicines with high precision.

When positioning the electrokinetic and related strategies for EVs analysis together with other commonly used methods, the electrokinetic ones would have the advantage of high resolution. Nevertheless, they are still mostly at research stage and require for most of them further improvement of measurement reproducibility. To bring a fair view to readers, the limitations of other established techniques are also mentioned, including limited resolution and sensitivity for NTA and DLS, low throughput for TEM and limited multi-parameter capability for flow cytometer. Depending on the measurement requirements and available infrastructure,

a single instrument or a combination of techniques is generally used to zoom into target EVs. Electrokinetic and related strategies, while still needing to further mature in the near future, could be included in the list of the methods of choice for this purpose.

4. Conclusion remarks and perspectives

The potential of EVs as a source of prognostic or diagnostic biomarkers but also as drug nanocarriers or gene therapy tools has attracted significant attention over the recent years. However, many technical challenges should be taken into account when dealing with such vesicles, notably their high heterogeneity, their small sizes, their fragility and also the tendency to aggregate or lyse. To date, ultracentrifugation (highest EV purity, lowest EV yield), commercial kits of polymer precipitation (highest EV yield, lowest EV purity) and SEC (compromise between purity and yield) are still the methods of choice for EVs isolation. For EV analysis, NTA, DLS, flow cytometry and TEM are the most widely used techniques. Electrokinetic strategies, together with microfluidic ones, bring not only new functionalities but also more possibilities of integration. They constitute an emerging trend that is expected soon to be ranked among the list of preferred methods for EVs isolation and analysis.

As reviewed here, there are different electrokinetically driven methods for isolation, preconcentration and separation of EVs. Most of them are still at the stage of research development (with an exception for TRPS). Application of such strategies on clinical samples and systematic comparison of their performances to those of established techniques still need to be investigated. Although some of electrokinetic approaches demonstrated their ability to distinguish subpopulation of EVs, results are highly variable according to how samples are handled or collected, storage conditions and on the measurement itself. Further improvement of the measurement reproducibility and precision is prerequisite. Although the current electrokinetic methods are unable to fully combine purification, enrichment, separation and

576 detection of EVs, they are individually capable of carrying out these steps quite efficiently as
577 discrete modules. Thus, we expect in the future the emergence of integrated electrokinetic
578 systems into a single platform to perform all these steps from highly complex biofluids. This
579 is indeed a positive feature (*i.e.* performing EVs isolation and analysis with a high degree of
580 automation, integration and ease of use) that electrokinetic strategies can address and make
581 them afterwards superior to more conventional methods. All these developments require
582 however the use of high-quality EV standards with narrow size distribution and homogeneous
583 population to reduce discrepancies and enable unbiased devices comparison. The generation
584 of recombinant EVs as a biological reference may open the door for well-characterized EV
585 standards [88], and should be used as the starting material for further development of
586 electrokinetic strategies for EVs isolation and analysis.
587
588
589
590 **Acknowledgement**
591 This work has been financially supported by the Institut Universitaire de France (for M.
592 Taverna, senior member). The doctoral scholarship for Marco Morani was supported by the
593 doctoral school 2MIB (Sciences Chimiques: Molécules, Matériaux, Instrumentation et
594 Biosystèmes) – University Paris Saclay.
595 The authors have declared no conflict of interest.
596
597
598
599
600

Table 1: Summary of the most commonly used EVs isolation techniques and their advantages / disadvantages.

Method	Advantages	Disadvantages
Ultracentrifugation	• Most commonly used • High purity by density gradient centrifugation	• High equipment cost • Time consuming • Large sample volume needed • Potential vesicle aggregation and mechanical damage • Low yield
Ultrafiltration	• Low equipment cost • Quick and simple • Possibility of processing many samples simultaneously	• Possible loss of vesicles due to clogging • Potential vesicle deterioration and deformation
Polymer-based precipitation	• Low cost • No special equipment required • High yield	• Co-precipitation of protein aggregates and polymeric contaminants • Low purity • Required clean-up steps
Size-exclusion chromatography	• Keep native structure of vesicles • High purity • Good reproducibility	• Limitation on sample volume • Long run time • Specific columns required
Immunoaffinity capture	• High purity • High efficiency for specific EV subtypes	• High reagent cost • Extra step for elution may damage EVs' native structure • Antibody cross-reactivity • Low yield

609

610 **Table 2:** Summary of commonly used EVs characterization techniques and their advantages /
611 disadvantages.

Method	Advantages	Disadvantages
Transmission electron microscopy (TEM)	• Direct assessment of morphology and size • Powerful magnification and resolution	• Laborious sample preparation • Time consuming • Expensive equipment
Dynamic light scattering (DLS)	• Fast • No need for sample preparation	• Inaccurate with polydisperse and size-heterogeneous samples
Nanoparticle tracking analysis (NTA)	• Ability to analyse normal and fluorescent samples • Approximate particle counts	• Contamination caused by diluents during the preparation of samples • Results are operator-dependent
Flow cytometry	• Single EV molecular characterization • Quantitative and qualitative	• Detection limit is flow dependent • Aggregates or debris can give false results • Technical expertise required
Tuneable resistive pulse sensing (TRPS)	• Particle by particle measurement of size and charge	• Difficult to select the correct nanopore setup • Possible pore clogging

		• Less reproducible

612

613 **Table 3:** Electrokinetic strategies for isolation and enrichment of EVs

EV isolation approach	Sample type	Recovery yield (%)	Isolation throughput (µL/min)	Isolated size (nm)	Ref
Electrophoresis-driven filtration	Mouse whole blood	1.5	2	150	[57]
Electrophoretic isolation on porous membrane	Mouse plasma	65	20	~ 10 - 400	[58]
Ion-depletion zone	Cell culture filtered EVs	98	1	not communicated	[59]
Ion concentration polarization (ICP)-based gel electrophoresis	Cell culture supernatant, blood serum	60 - 80	2.5 - 3.5	≤ 150	[61]
Ion concentration polarization (ICP)-based electrokinetic concentrator	Cell culture supernatant	not communicated	1	~ 50 - 75	[62]
alternating current electrohydrodynamic (ac-EHD) induced nanoshearing	Exosome pellets from breast and prostate cancer cell lines	not communicated	not communicated	30–350	[63]

614

615

616

617

618
619
620
621
622
623
624
625
626
627
628
629
630
631
632
633

634 **Table 4:** Electrokinetic strategies for separation and quantification of EVs

EV analysis approach	Sample type	Detection limit	Calibration range	Operation time	Isolated size (nm)	Concentration (particles / mL)	Ref
Alternating current electrokinetic (ACE) microarray chip	glioblastoma EVs purified from cell culture and spiked in human plasma	not communicated	not communicated	< 30 min	~ 50 – 150 (UC)	~ 1–10 × 10^9 (loaded into the system)	[69]
Alternating current electrokinetic (ACE) microarray chip	EVs from whole blood, plasma and serum of pancreatic ductal adenocarcinoma (PDAC) patients	not communicated	not communicated	< 30 min	~ 20 - 500	not communicated	[70]
Nanopipette insulator-based dielectrophoresis (iDEP) device	EVs extracted from plasma of healthy donors and resuspended in PBS	not communicated	not communicated	~ 2 min (only for entrapment)	not communicated	not communicated	[71]
Nanopipette insulator-based dielectrophoresis (iDEP) device (four pipettes in parallel)	EVs from undiluted human plasma, serum and saliva	not communicated	not communicated	20 min (10 min entrapment and 10 min collection)	50 – 150	1.01 × 10^{12} (detected after isolation)	[72]
Direct current–insulator-based dielectrophoretic (DC-iDEP) system	EVs purified from human breast adenocarcinoma cells	not communicated	not communicated	20 s (for entrapment and separation)	~ 75 (section 2); ~ 120 (section 1)	2.1 × 10^{10} (loaded into the system)	[73, 74]
Dielectrophoresis (DEP) chip	EVs isolated from plasma of lung cancer patients	not communicated	not communicated	30 min	~ 50 - 250	7.13 ± 0.86 × 10^{10} (detected after isolation)	[75]
On-chip microcapillary electrophoresis (μCE) coupled with a laser dark-field microscope	EVs extracted from six types of human cell	not communicated	not communicated	not communicated	not communicated	not communicated	[76]
On-chip microcapillary electrophoresis (μCE) coupled with a laser dark-field microscope	EVs extracted from normal and cancer prostate cells	not communicated	not communicated	not communicated	not communicated	not communicated	[77]
On-chip microcapillary electrophoresis (μCE) coupled with a laser dark-field microscope + immunoelectrophoresis	EVs collected from culture supernatant of human breast cancer cells and from mouse blood	not communicated	not communicated	not communicated	~ 50 – 450 (UC)	1.19×10^{12} (loaded into the system)	[78]
Capillary electrophoresis (CE) coupled with UV-	EVs isolated from human urine	not communicated	not communicated	~ 4 h (separation)	80 – 120 (low density EVs);	not communicated	[80]

visible detector					40 – 100 (heavy density EVs) (Sucrose gradient UC)		
Capillary electrophoresis (CE) coupled with UV-visible detector	EVs isolated from *Pectobacterium betavasculorum* strain	protein concentration down to 0.17 mg/mL		< 15 min (separation)	< 200 (differential centrifugation + filtration)	not communicated	[81]
Capillary electrophoresis coupled with laser-induced fluorescent (LIF) detection	EVs isolated from bovine milk, pony plasma/serum and human plasma	8×10^9 EVs / mL	1.22×10^{10} to 1.20×10^{11} EVs / mL	< 30 min (separation)	< 200 (sucrose gradient UC, size exclusion chromatography, monolithic affinity chromatography)		[47]
Cyclical electrical field flow fractionation (Cy-El-FFF)	EVs purified from human melanoma cells	not communicated	not communicated	not communicated	~ 120 (radius) (differential centrifugation)	not communicated	[45]
Capacitance-voltage measurements	EVs isolated from human embryonic kidney cell line and small cell lung cancer cell line	not communicated	not communicated	10 min	90 – 110 (ExoQuick-TC kit)	$> 1 \times 10^6$	[83]

Figure captions:

Fig. 1. *Schematic representation of the different types of membrane vesicles released by cells, either by direct budding from the plasma membrane (PM) or by fusion of internal multivesicular compartments (MVB) with the PM. Reprinted from [89] with permission. Copyright (2014) Annual Reviews.*

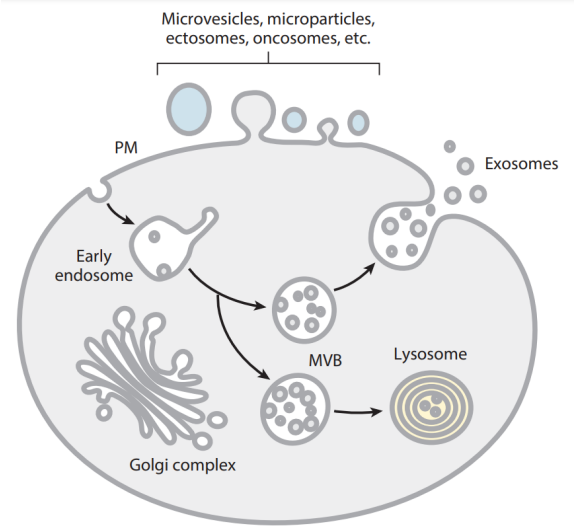

Fig. 2. *Schematic drawings for electrokinetically driven methods for (A) EVs isolation; and (B) EVs separation and characterization.*

A)

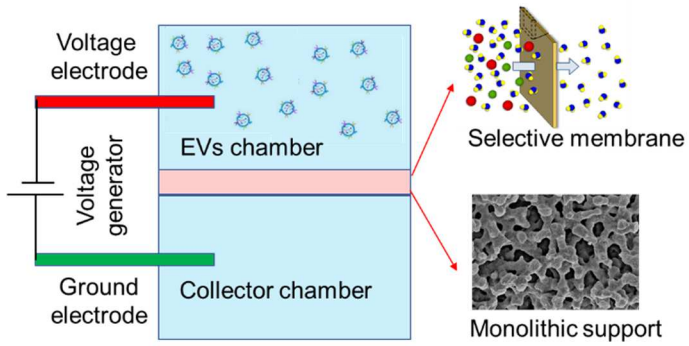

B)

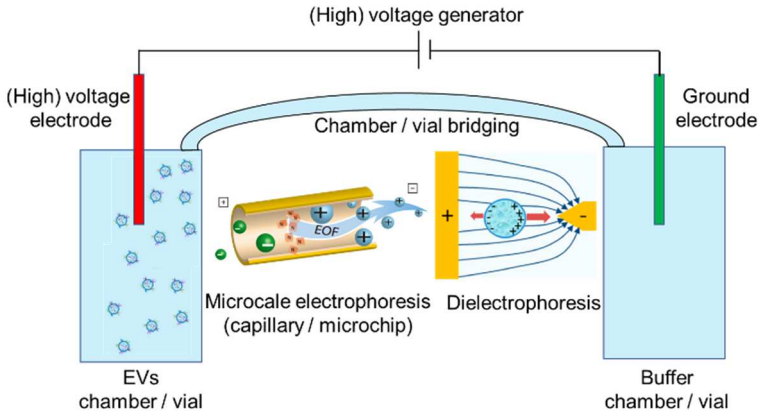

Fig. 3. *(a) Schematic drawing of pressure-driven filtration procedure. Inlet pressure bias drives particles through the membrane into the collection chamber. After injection of the blood sample, the filtrate is collected by injecting one chamber volume of PBS through the collection inlet to eject the permeated EVs. ''X'' indicates an outlet blocked by sealing the attached plastic tubing. (b) Schematic of electrophoresis-driven filtration. Bias voltage is applied across the porous polymer monolith (PPM) membrane so that negatively charged vesicles experience a transmembrane driving force. Filtration is performed under syringe pump driven flow. 10 V is applied over an electrode separation distance of 1.5 cm for an electric field strength of 6.7 V/cm. Reprinted from [57] with permission. Copyright (2012) RSC.*

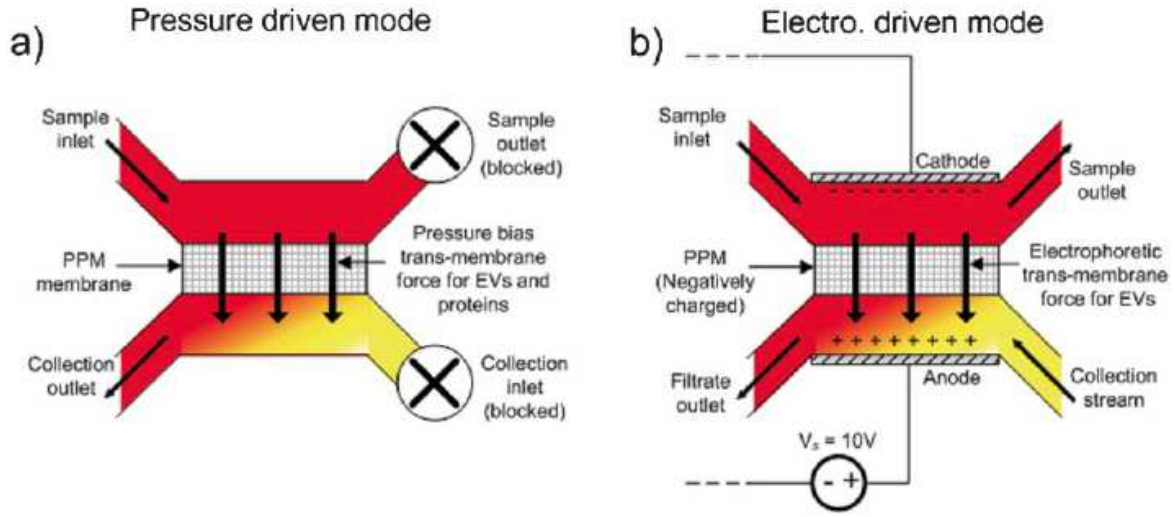

Fig. 4. *Schematic drawing of the generation of an ion-depletion zone for EVs preconcentration. An ion-depletion zone is formed by applying a voltage between two microchannels bridged by an ion-exchange membrane. (1) Cations that are drawn into and anions are pushed away from the edge of the Nafion membrane on the high-voltage side by an electrostatic force. (2) The generated ion-depletion zone is used as an intangible barrier against the entry of charged particles. A Nafion pattern intersects the Main and the GND channels. The inlet and outlet ports of the channels are in contact with the electrodes to apply an electric potential difference between the two microchannels. Reprinted from [59] with permission. Copyright (2018) JSAC.*

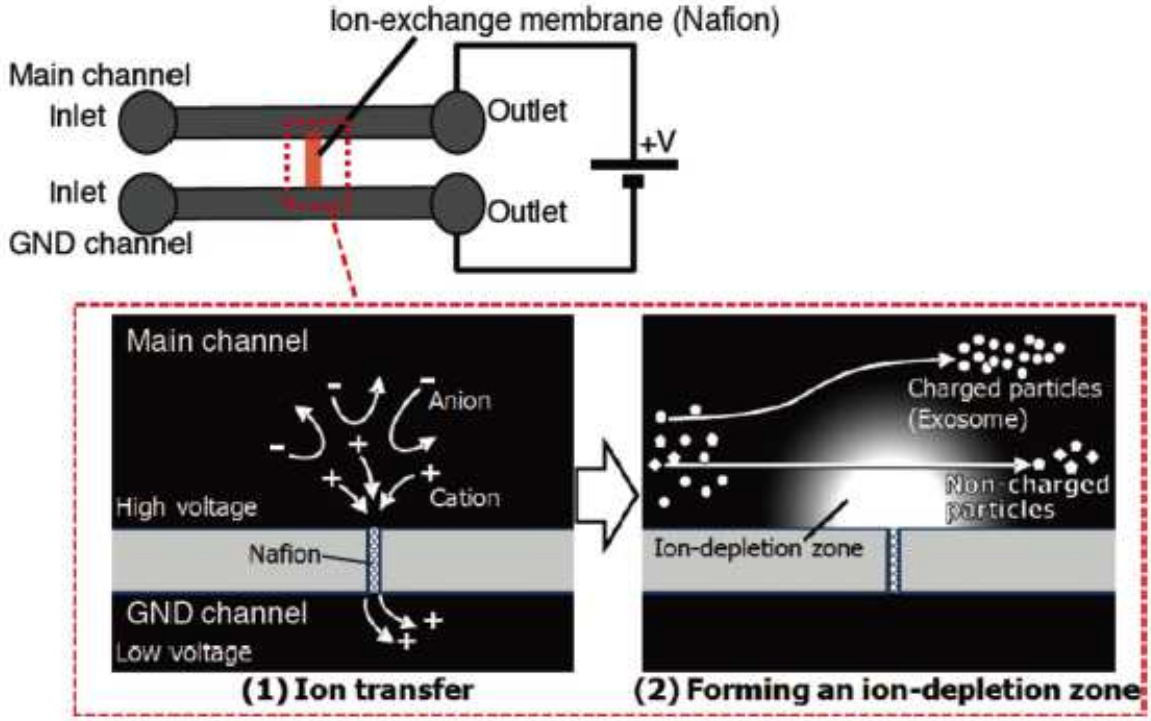

Fig. 5. *Schematic drawing (A) as well as simulated and captured photos (B) of the microelectrode array chip showing the cross-sectional and top views of a single electrode. Over 1000 electrodes can be set in a single device. The DEP high-field regions where particles are collected are shown within the dotted lines. The darker color of the silicon dioxide layer and electrode in the top view represents the overlying transparent porous hydrogel layer. Reprinted from [69] with permission. Copyright (2017) ACS.*

(A)

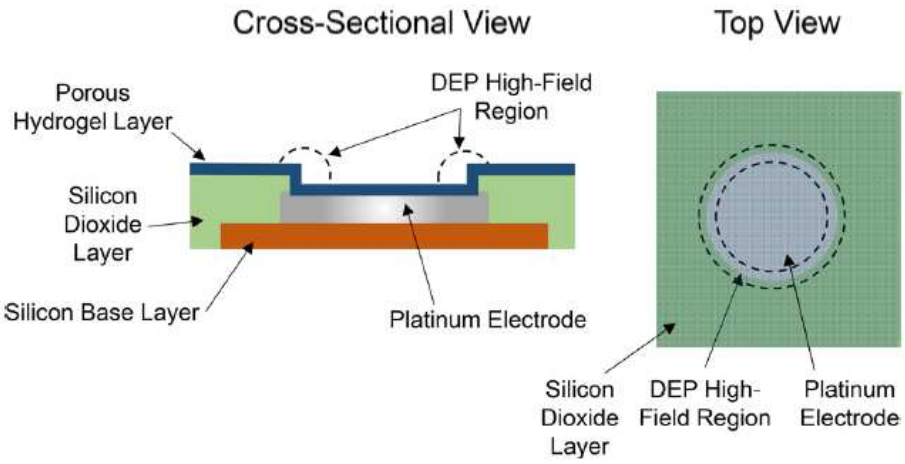

(B)

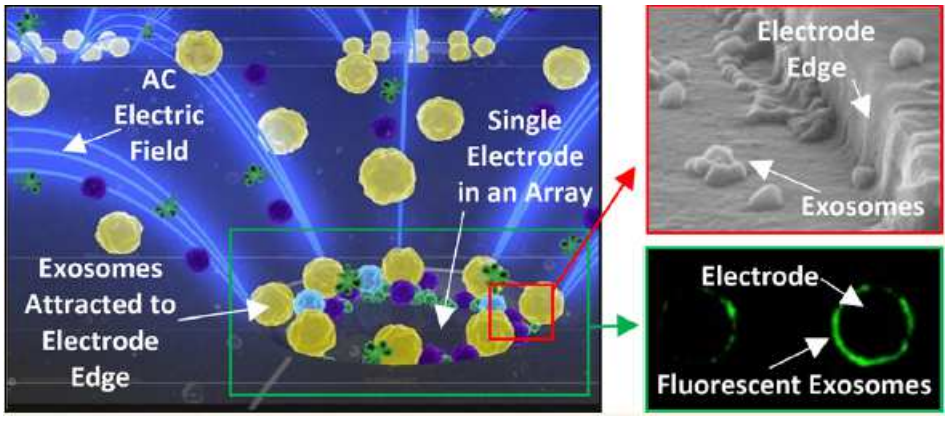

Fig. 6. *(A) Schematic drawing of the nanopipette DEP device for entrapment of the particles suspended in the solution. (B) The overall setup. The ionic current across the pipette and the trajectory of the particles were simultaneously recorded. DEP stands for dielectrophoresis; EP and EOF stand for electrophoresis and electroosmotic flow, respectively. Reprinted from [71] with permission. Copyright (2018) Nature.*

(A)

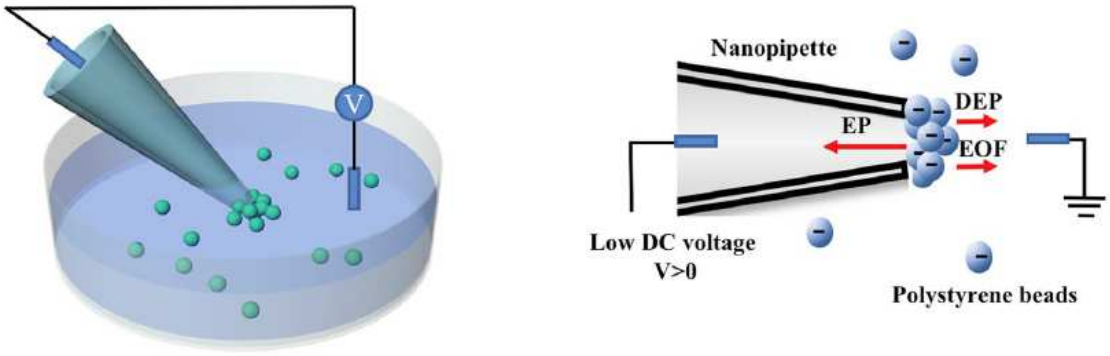

(B)

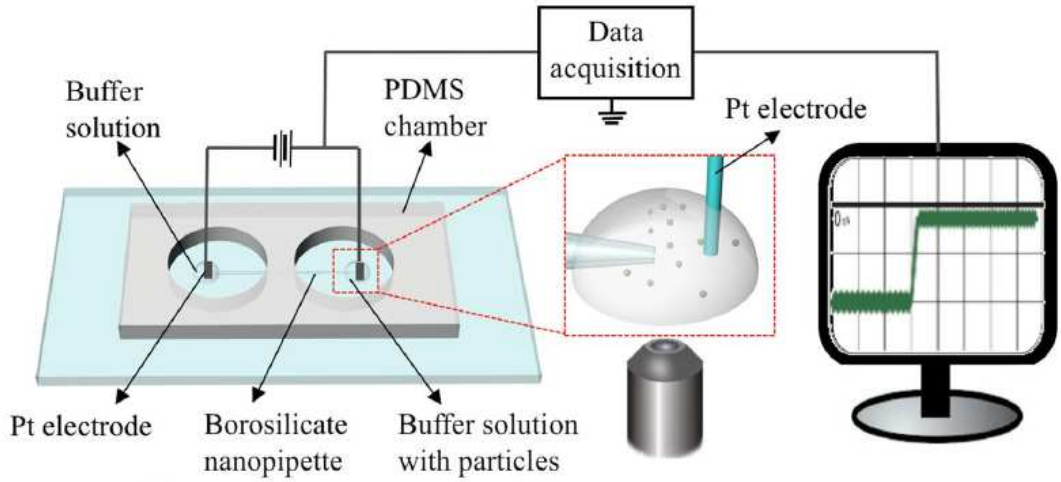

Fig. 7. *(a) Schematic drawing of the on-chip μCE system with a laser dark-field microscope. The system consists of a μCE chip, a pair of platinum electrodes, a DC power supply, a laser source, an inverted microscope, and an EM-CCD camera. The μCE chip equipped with a microfluidic channel with small reservoir tanks on both ends and the platinum electrodes were mounted on the inverted microscope. (b) Dark-field image of exosomes. Reprinted from [76] with permission. Copyright (2013) IOPScience.*

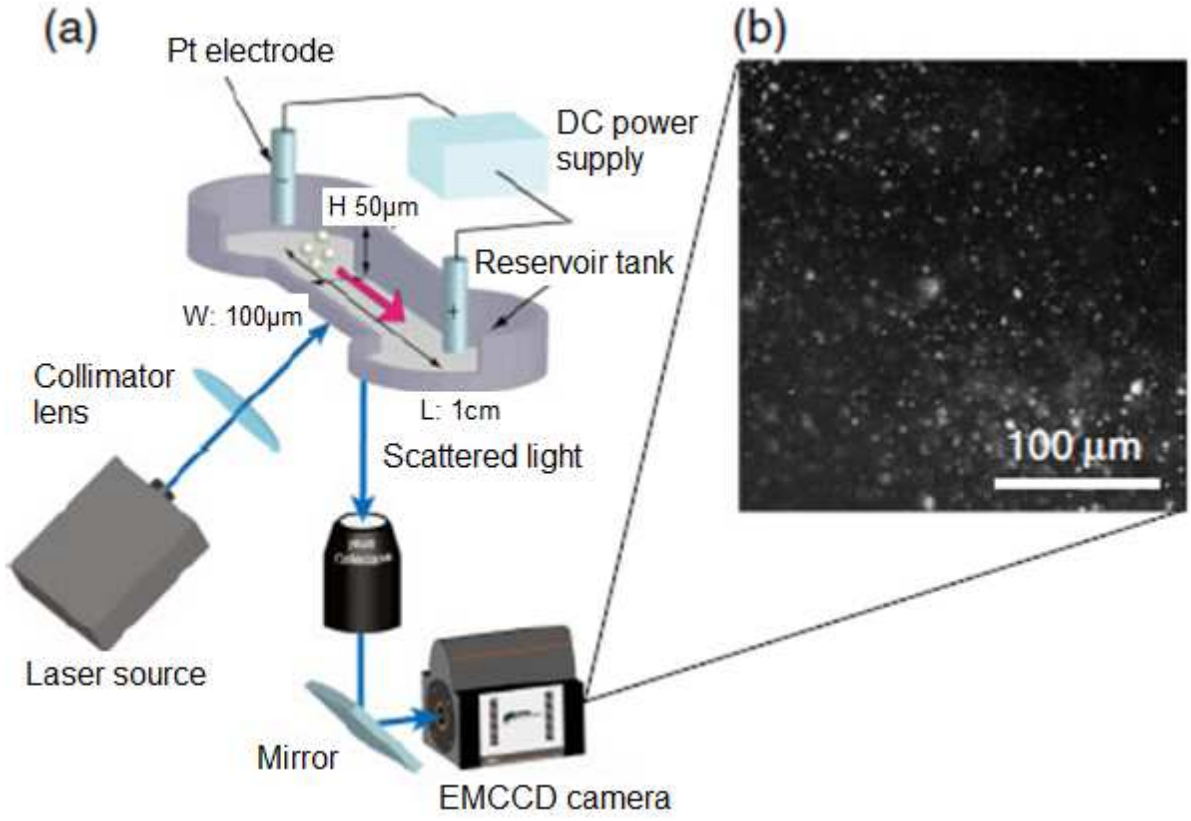

Fig. 8. *Work flow of the CE-LIF method for separation and quantification of fluorescent EVs via intra-membrane labelling approach. CFDA-SE: 5-(and-6)-Carboxyfluorescein diacetate succinimidyl ester dye. Reprinted from [47] with permission. Copyright (2020) Elsevier.*

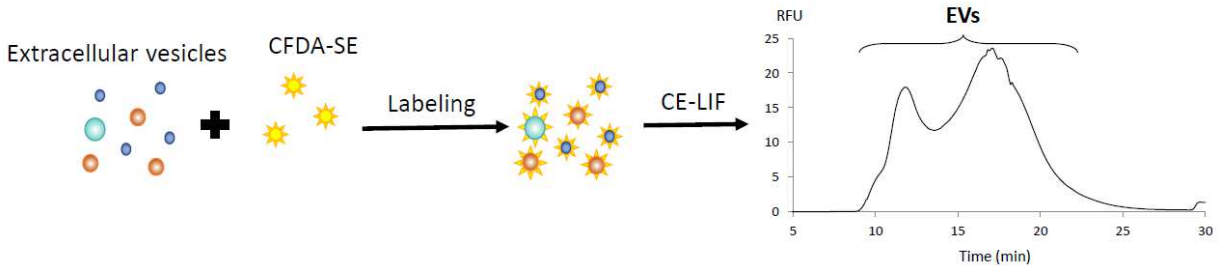

References:

[1] K.W. Witwer, C. Théry, J. Extracell. Vesicles 8 (2019) 1648167.

[2] C. Thery, K.W. Witwer, E. Aikawa, *et al*., J. Extracell. Vesicles 7 (2018) 43.

[3] M. Yanez-Mo, P.R.M. Siljander, Z. Andreu, *et al*., J. Extracell. Vesicles 4 (2015) 60.

[4] N. Iraci, T. Leonardi, F. Gessler, B. Vega, S. Pluchino, Int. J. Mol. Sci. 17 (2016) 32.

[5] G. van Niel, G. D'Angelo, G. Raposo, Nat. Rev. Mol. Cell Biol 19 (2018) 213.

[6] A. Latifkar, R.A. Cerione, M.A. Antonyak, Biochem. Soc. Trans. 46 (2018) 1137.

[7] A. Latifkar, Y.H. Hur, J.C. Sanchez, R.A. Cerione, M.A. Antonyak, J. Cell Sci. 132 (2019) 9.

[8] A. Becker, B.K. Thakur, J.M. Weiss, H.S. Kim, H. Peinado, D. Lyden, Cancer Cell 30 (2016) 836.

[9] R.E. Lane, D. Korbie, M.M. Hill, M. Trau, Clin. Transl. Med. 7 (2018) 11.

[10] H.C. Bu, D.G. He, X.X. He, K.M. Wang, Chembiochem 20 (2019) 451.

[11] J. Howitt, A.F. Hill, J. Biol. Chem. 291 (2016) 26589.

[12] M.H. Rashed, E. Bayraktar, G.K. Helal, M.F. Abd-Ellah, P. Amero, A. Chavez-Reyes, C. Rodriguez-Aguayo, Int. J. Mol. Sci. 18 (2017) 25.

[13] R.C. Lai, R.W.Y. Yeo, K.H. Tan, S.K. Lim, Biotech. Adv. 31 (2013) 543.

[14] M.J. Haney, N.L. Klyachko, Y.L. Zhaoa, R. Gupta, E.G. Plotnikova, Z.J. He, T. Patel, A. Piroyan, M. Sokolsky, A.V. Kabanov, E.V. Batrakova, J. Control. Release 207 (2015) 18.

[15] F. Menay, L. Herschlik, J. De Toro, F. Cocozza, R. Tsacalian, M.J. Gravisaco, M.P. Di Sciullo, A. Vendrell, C.I. Waldner, C. Mongini, Frontiers in Immunology 8 (2017) 14.

[16] Y. Wang, Y.R. Zhang, G. Cai, Q. Li, Int. J. Nanomed. 15 (2020) 4257.

[17] D.S. Choi, D.K. Kim, Y.K. Kim, Y.S. Gho, Proteomics 13 (2013) 1554.

[18] X.X. Yang, C. Sun, L. Wang, X.L. Guo, J. Control. Release 308 (2019) 119.

[19] D. Yang, W. Zhang, H. Zhang, F. Zhang, L. Chen, L. Ma, L.M. Larcher, S. Chen, N. Liu, Q. Zhao, P.H.L. Tran, C. Chen, R.N. Veedu, T. Wang, Theranostics 10 (2020) 3684.

[20] B.Y. Chen, C.W.H. Sung, C.C. Chen, C.M. Cheng, D.P.C. Lin, C.T. Huang, M.Y. Hsu, Clin. Chim. Acta 493 (2019) 14.

[21] H.L. Shao, H. Im, C.M. Castro, X. Breakefield, R. Weissleder, H.H. Lee, Chem. Rev. 118 (2018) 1917.

[22] W.S. Wang, J. Luo, S.T. Wang, Adv. Healthcare Mater. 7 (2018).

[23] P. Li, M. Kaslan, S.H. Lee, J. Yao, Z.Q. Gao, Theranostics 7 (2017) 789.

[24] M.Y. Konoshenko, E.A. Lekchnov, A.V. Vlassov, P.P. Laktionov, Biomed. Res. Int. (2018) 27.

[25] T.S. Martins, J. Catita, I.M. Rosa, O. Silva, A.G. Henriques, Plos One 13 (2018).

[26] M.I. Ramirez, M.G. Amorim, C. Gadelha, I. Milic, J.A. Welsh, V.M. Freitas, M. Nawaz, N. Akbar, Y. Couch, L. Makin, F. Cooke, A.L. Vettore, P.X. Batista, R. Freezor, J.A. Pezuk, L. Rosa-Fernandes, A.C.O. Carreira, A. Devitt, L. Jacobs, I.T. Silva, G. Coakley, D.N. Nunes, D. Carter, G. Palmisano, E. Dias-Neto, Nanoscale 10 (2018) 881.

[27] C. Gardiner, D. Di Vizio, S. Sahoo, C. Thery, K.W. Witwer, M. Wauben, A.F. Hill, J. Extracell. Vesicles 5 (2016).

[28] K. Brennan, K. Martin, S. FitzGerald, J. O'Sullivan, Y. Wu, A. Blanco, C. Richardson, M. Mc Gee, Sci. Rep. 10 (2020) 1.

[29] S. Gholizadeh, M.S. Draz, M. Zarghooni, A. Sanati-Nezhad, S. Ghavami, H. Shafiee, M. Akbari, Biosens. Bioelectron. 91 (2017) 588.

[30] W.T. Su, H.J. Li, W.W. Chen, J.H. Qin, Trac-Trends Anal. Chem. 118 (2019) 686.

[31] Y. Jia, Z.H. Ni, H. Sun, C. Wang, Ieee Access 7 (2019) 45080.

[32] S.J. Lin, Z.X. Yu, D. Chen, Z.G. Wang, J.M. Miao, Q.C. Li, D.Y. Zhang, J. Song, D.X. Cui, Small 16 (2020).

[33] A. Liga, A.D.B. Vliegenthart, W. Oosthuyzen, J.W. Dear, M. Kersaudy-Kerhoas, Lab Chip 15 (2015) 2388.

[34] U. Erdbrugger, J. Lannigan, Cytometry Part A 89A (2016) 123.

[35] R. Szatanek, M. Baj-Krzyworzeka, J. Zimoch, M. Lekka, M. Siedlar, J. Baran, Int. J. Mol. Sci. 18 (2017).

[36] J.C. Contreras-Naranjo, H.J. Wu, V.M. Ugaz, Lab Chip 17 (2017) 3558.

[37] L. Trapiella-Alfonso, G. Ramirez-Garcia, F. d'Orlye, A. Varenne, Trac-Trends Anal. Chem. 84 (2016) 121.

[38] M.N. Alves, M. Miro, M.C. Breadmore, M. Macka, Trac-Trends Anal. Chem. 114 (2019) 89.

[39] S. Dziomba, K. Ciura, M. Dawid, J. Chromatogr. A 1606 (2019).

[40] T.K. Mudalige, H. Qu, D. Van Haute, S.M. Ansar, S.W. Linder, Trac-Trends Anal. Chem. 106 (2018) 202.

[41] S. Gill, R. Catchpole, P. Forterre, FEMS Microbiol. Rev. 43 (2019) 273.

[42] J. Kowal, G. Arras, M. Colombo, M. Jouve, J.P. Morath, B. Primdal-Bengtson, F. Dingli, D. Loew, M. Tkach, C. Thery, PNAS 113 (2016) E968.

[43] L. Margolis, Y. Sadovskyz, Plos Biology 17 (2019) 12.

[44] I. Parolini, C. Federici, C. Raggi, L. Lugini, S. Palleschi, A. De Milito, C. Coscia, E. Iessi, M. Logozzi, A. Molinari, M. Colone, M. Tatti, M. Sargiacomo, S. Fais, J. Biol. Chem. 284 (2009) 34211.

[45] K.E. Petersen, F. Shiri, T. White, G.T. Bardi, H. Sant, B.K. Gale, J.L. Hood, Anal. Chem. 90 (2018) 12783.

[46] A. Zijlstra, D. Di Vizio, Na. Cell Biol. 20 (2018) 228.

[47] M. Morani, T.D. Mai, Z. Krupova, P. Defrenaix, E. Multia, M.-L. Riekkola, M. Taverna, Anal. Chim. Acta (2020).

[48] V.S. Chernyshev, R. Rachamadugu, Y.H. Tseng, D.M. Belnap, Y.L. Jia, K.J. Branch, A.E. Butterfield, L.F. Pease, P.S. Bernard, M. Skliar, Anal. Bioanal. Chem. 407 (2015) 3285.

[49] J.H. Deng, Z.J. Li, Z.X. Wang, J. Feng, X.J. Huang, Z.M. Zeng, Microscopy and Microanal. 26 (2020) 310.

[50] F. Cao, Y. Gao, Q. Chu, Q. Wu, L. Zhao, T. Lan, L. Zhao, Electrophoresis (2019) 7.

[51] F. d'Orlye, A. Varenne, P. Gareil, Electrophoresis 29 (2008) 3768.

[52] F. d'Orlye, A. Varenne, T. Georgelin, J.M. Siaugue, B. Teste, S. Descroix, P. Gareil, Electrophoresis 30 (2009) 2572.

[53] F.K. Liu, F.H. Ko, P.W. Huang, C.H. Wu, T.C. Chu, J. Chromatogr. A 1062 (2005) 139.

[54] N.G. Vanifatova, B.Y. Spivakov, J. Mattusch, U. Franck, R. Wennrich, Talanta 66 (2005) 605.

[55] U. Pyell, Electrophoresis 31 (2010) 814.

[56] H.K. Jones, N.E. Ballou, Anal. Chem. 62 (1990) 2484.

[57] R.T. Davies, J. Kim, S.C. Jang, E.J. Choi, Y.S. Gho, J. Park, Lab Chip 12 (2012) 5202.

[58] S. Cho, W. Jo, Y. Heo, J.Y. Kang, R. Kwak, J. Park, Sens. Actuators B 233 (2016) 289.

[59] K. Mogi, K. Hayashida, T. Yamamoto, Anal. Sci. 34 (2018) 875.

[60] J. Kim, S. Sahloul, A. Orozaliev, V.Q. Do, V.S. Pham, D. Martins, X. Wei, R. Levicky, Y.A. Song, IEEE Nanotechnol. Mag. 14 (2020) 18.

[61] S. Marczak, K. Richards, Z. Ramshani, E. Smith, S. Senapati, R. Hill, D.B. Go, H.C. Chang, Electrophoresis 39 (2018) 2029.

[62] L.S. Cheung, S. Sahloul, A. Orozaliev, Y.A. Song, Micromachines 9 (2018) 12.

[63] R. Vaidyanathan, M. Naghibosadat, S. Rauf, D. Korbie, L.G. Carrascosa, M.J.A. Shiddiky, M. Trau, Anal. Chem. 86 (2014) 11125.

[64] Y. Tian, M.F. Gong, Y.Y. Hu, H.S. Liu, W.Q. Zhang, M.M. Zhang, X.X. Hu, D. Aubert, S.B. Zhu, L. Wu, X.M. Yan, J. Extracell. Vesicles 9 (2020).

[65] H.A. Pohl, Journal of Applied Physics 22 (1951) 869.

[66] R. Pethig, Biomicrofluidics 4 (2010) 35.

[67] A. Kuzyk, Electrophoresis 32 (2011) 2307.

[68] C. Qian, H.B. Huang, L.G. Chen, X.P. Li, Z.B. Ge, T. Chen, Z. Yang, L.N. Sun, Int. J. Mol. Sci. 15 (2014) 18281.

[69] S.D. Ibsen, J. Wright, J.M. Lewis, S. Kim, S.Y. Ko, J. Ong, S. Manouchehri, A. Vyas, J. Akers, C.C. Chen, B.S. Carter, S.C. Esener, M.J. Heller, Acs Nano 11 (2017) 6641.

[70] J.M. Lewis, A.D. Vyas, Y.Q. Qiu, K.S. Messer, R. White, M.J. Heller, Acs Nano 12 (2018) 3311.

[71] L.L. Shi, A. Rana, L. Esfandiari, Sci. Rep. 8 (2018) 12.

[72] L.L. Shi, D. Kuhnell, V.J. Borra, S.M. Langevin, T. Nakamura, L. Esfandiari, Lab Chip 19 (2019) 3726.

[73] S. Ayala-Mar, R.C. Gallo-Villanueva, J. Gonzalez-Valdez, Materials Today - Proceedings 13 (2019) 332.

[74] S. Ayala-Mar, V.H. Perez-Gonzalez, M.A. Mata-Gomez, R.C. Gallo-Villanueva, J. Gonzalez-Valdez, Anal. Chem. 91 (2019) 14975.

[75] J.G. Chen, Y.C. Xu, X. Wang, D.C. Liu, F. Yang, X.R. Zhu, Y. Lu, W.L. Xing, Lab on a Chip 19 (2019) 432.

[76] K. Kato, M. Kobayashi, N. Hanamura, T. Akagi, N. Kosaka, T. Ochiya, T. Ichiki, Jpn. J. Appl. Phys. 52 (2013) 4.

[77] T. Akagi, K. Kato, N. Hanamura, M. Kobayashi, T. Ichiki, Jpn. J. Appl. Phys. 53 (2014).

[78] T. Akagi, K. Kato, M. Kobayashi, N. Kosaka, T. Ochiya, T. Ichiki, Plos One 10 (2015) e0123603.

924 [79] T. Akagi, T. Ichiki, in: W.P. Kuo and S. Jia (Eds.), Microcapillary Chip-Based
925 Extracellular Vesicle Profiling System, Humana Press Inc. Totowa, 2017, pp. 209.
926 [80] T. Lan, X. Xi, Q. Chu, L. Zhao, A. Chen, J.J. Lu, F. Wang, W. Zhang, Electrophoresis 39
927 (2018) 2316.
928 [81] M. Piotrowska, K. Ciura, M. Zalewska, M. Dawid, B. Correia, P. Sawicka, B. Lewczuk,
929 J. Kasprzyk, L. Sola, W. Piekoszewski, B. Wielgomas, K. Waleron, S. Dziomba, J.
930 Chromatogr. A (2020) 461047.
931 [82] Y. Tani, T. Kaneta, J. Chromatogr. A 1629 (2020) 461513.
932 [83] M. Al Ahmad, Ieee Access 6 (2018) 22817.
933 [84] A. Akbarinejad, C.L. Hisey, D. Brewster, J. Ashraf, V. Chang, S. Sabet, Y. Nursalim, V.
934 Lucarelli, C. Blenkiron, L. Chamley, D. Barker, D.E. Williams, C.W. Evans, J. Travas-
935 Sejdic, ACS Appl. Mater. Interfaces 12 (2020) 39005.
936 [85] R. Vogel, G. Willmott, D. Kozak, G.S. Roberts, W. Anderson, L. Groenewegen, B.
937 Glossop, A. Barnett, A. Turner, M. Trau, Anal. Chem. 83 (2011) 3499.
938 [86] D. Kozak, W. Anderson, R. Vogel, S. Chen, F. Antaw, M. Trau, ACS Nano 6 (2012)
939 6990.
940 [87] qNano, IZON https://store.izon.com/collections/instruments/products/qnano-gold (2020).
941 [88] E. Geeurickx, J. Tulkens, B. Dhondt, J.V. Deun, L. Lippens, G. Vergauwen, E. Heyrmari,
942 D. De Sutter, K. Gevaert, F. Impens, I. Miinalainen, P.J. Van Bockstal, T. De Beer,
943 M.H.M. Wauben, E.N.M. Nolte-'t-Hoen, K. Bloch, J.V. Swinnen, E. van der Pol, R.
944 Nieuwland, G. Braems, N. Callewaert, P. Mestdagh, J. Vandesompele, H. Denys, S.
945 Eyckerman, O. De Wever, A. Hendrix, Nat. Commun. 10 (2019).
946 [89] M. Colombo, G. Raposo, C. Thery, in: R. Schekman and R. Lehmann (Eds.), Biogenesis,
947 Secretion, and Intercellular Interactions of Exosomes and Other Extracellular Vesicles.
948 2014, pp. 255.